



## Genesis and Evolution of the 1997-98 El Niño

Michael J. McPhaden, *et al.*

*Science* **283**, 950 (1999);

DOI: 10.1126/science.283.5404.950

**The following resources related to this article are available online at [www.sciencemag.org](http://www.sciencemag.org) (this information is current as of February 6, 2007):**

**Updated information and services**, including high-resolution figures, can be found in the online version of this article at:

<http://www.sciencemag.org/cgi/content/full/283/5404/950>

This article has been **cited by** 366 article(s) on the ISI Web of Science.

This article has been **cited by** 13 articles hosted by HighWire Press; see:

<http://www.sciencemag.org/cgi/content/full/283/5404/950#otherarticles>

This article appears in the following **subject collections**:

Atmospheric Science

<http://www.sciencemag.org/cgi/collection/atmos>

Information about obtaining **reprints** of this article or about obtaining **permission to reproduce this article** in whole or in part can be found at:

<http://www.sciencemag.org/help/about/permissions.dtl>



# Genesis and Evolution of the 1997–98 El Niño

Michael J. McPhaden

The 1997–98 El Niño was, by some measures, the strongest on record, with major climatic impacts felt around the world. A newly completed tropical Pacific atmosphere-ocean observing system documented this El Niño from its rapid onset to its sudden demise in greater detail than was ever before possible. The unprecedented measurements challenge existing theories about El Niño-related climate swings and suggest why climate forecast models underpredicted the strength of the El Niño before its onset.

One of the major accomplishments of the 10-year (1985–94) Tropical Ocean Global Atmosphere (TOGA) program was the implementation of a new observing system for oceanic and atmospheric measurements to improve description, understanding, and prediction of El Niño–Southern Oscillation (ENSO) variability (1). This “ENSO Observing System,” consisting of satellite and in situ measurements (2), was fully in place in time to capture the 1997–98 El Niño. The new data provided not only the most comprehensive description to date of a major El Niño event, but also led to improved long-range seasonal weather forecasts around the globe (3, 4). The data from this observing system, and in particular from the Tropical Atmosphere Ocean (TAO) array of moored buoys (5), are presented here to describe the evolution of the 1997–98 El Niño and highlight the oceanic and atmospheric processes that gave rise to it.

A weakening and reversal of the trade winds in the western and central equatorial Pacific led to the rapid development of unusually warm sea-surface temperatures (SSTs) east of the international date line in early 1997 (Figs. 1 and 2). The western Pacific warm pool (surface waters greater than about 29°C) migrated eastward with the collapse of the trade winds, and the equatorial cold tongue—the strip of cool water indicative of equatorial upwelling that normally occupies the eastern and central Pacific between the coast of South America to the international date line—failed to develop in boreal summer and fall 1997 (Figs. 1 and 3). The El Niño developed so rapidly that each month from June to December 1997 a new monthly record high was set for SST in the eastern equatorial Pacific, based on measure-

ments dating back to the middle of the last century (Fig. 4). At the height of the event in December 1997, 28° to 29°C water filled the equatorial basin (Figs. 1 and 3), and SST anomalies (that is, deviations from climatological norms) averaged nearly 4°C in the cold tongue region (6). These anomalies were the largest on record in the eastern equatorial Pacific (Fig. 4).

The development of El Niño conditions in the equatorial Pacific during 1997 was significantly modulated by higher frequency variability. Weakening and reversal of the trade winds in early 1997 were punctuated by a series of westerly wind events of generally increasing intensity or fetch along the equator (Figs. 1 and 2). These westerly episodes were the manifestation of the Madden-Julian oscillation (MJO), a wave in the atmosphere with

a 30- to 60-day period originating over the Indian Ocean (7). Deep atmospheric convection and low-level westerly winds associated with the MJO are usually observed only over relatively warm surface water. Consistent with these relationships, our observations indicate that the strongest surface westerly winds and deep convection were apparent only over waters warmer than about 29°C (Figs. 1 and 2).

Ocean currents forced by these westerly winds advected warm water eastward near the equator (8, 9). As a result, the warm pool expanded, increasing the areal extent of warm water over which subsequent cycles of the MJO could force the ocean. The amount of wind energy transferred from the atmosphere to the ocean depends in part on wind fetch, so that an eastward expansion of the warm pool resulted in a positive feedback between westerly wind forcing and the warm pool expansion (10). In addition, increasingly strong westerly wind forcing generated downwelling intraseasonal equatorial Kelvin waves of increasing amplitude. These waves propagated eastward across the basin in about 2 months, ultimately depressing the thermocline in the eastern Pacific by more than 90 m in late 1997 (Fig. 2). A depressed thermocline favors development of warm surface temper-

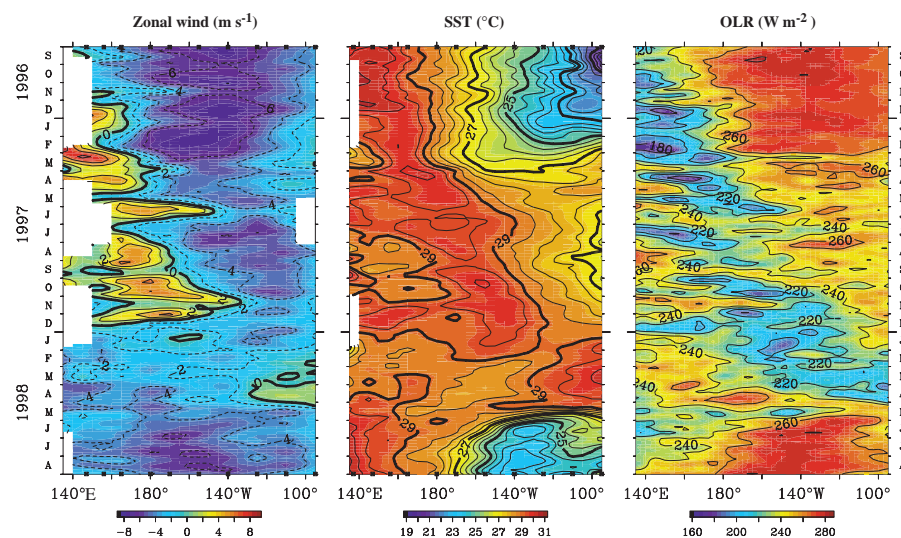


**Fig. 1.** Time versus longitude sections of surface zonal wind (left), SST (middle), and outgoing longwave radiation (OLR) (right) from September 1996 to August 1998. Analyses are based on 5-day averages for between 2°N and 2°S for the TAO data, and between 2.5°N and 2.5°S for OLR. Black squares on the abscissas of the wind and SST plots indicate longitudes of data availability at the start (top) and end (bottom) of the time-series record. Positive winds are westerly, negative winds are easterly. OLR values below about 235  $W m^{-2}$  indicate an increased likelihood of deep cumulus cloudiness and heavy convective precipitation. OLR data are from the National Centers for Environmental Prediction.

The author is at the National Oceanic and Atmospheric Administration (NOAA)/Pacific Marine Environmental Laboratory, 7600 Sand Point Way NE, Seattle, WA 98115, USA. E-mail: mcphaden@pmel.noaa.gov

atures, because the subsurface cold water reservoir that feeds upwelling in the equatorial cold tongue is pushed down to greater depths (11). In the western Pacific, on the other hand, the thermocline shoaled by 20 to 40 m in 1997 as Rossby waves excited by the initial weakening of the trade winds propagated westward toward Indonesia and New Guinea (12). SSTs cooled in the west, presumably because of enhanced evaporative heat loss from the ocean and greater oceanic mixing of cold subsurface waters due to MJO-generated ocean turbulence (13). The net result of these processes was a flattening of the thermocline and disappearance of the normal east-west SST gradient along the equator. The weakened large-scale SST gradient, in turn, fed back into a large-scale weakening of the trade winds, within which the series of westerly events was embedded.

In early 1998, SSTs in the eastern Pacific exceeded 29°C (Fig. 1) as warm anomalies were superimposed on the usual seasonal warming that occurs at this time of year (Fig. 5). Westerly wind anomalies, though weaker than earlier in the El Niño event, migrated eastward in tandem with the 29°C water. Thermocline shoaling, initially confined to west of the international date line, slowly progressed into the central and eastern Pacific. However, SSTs remained anomalously high east of the date line, because the local winds were weak there in early 1998 (Figs. 2 and 5). It was not until the trade winds abruptly returned to near normal strength in the eastern Pacific in mid-May 1998 that the cold subsurface waters could be efficiently upwelled. SSTs in the equatorial cold tongue then plummeted because of the close proximity of the thermocline to the surface. At one location (0°, 125°W), SST dropped 8°C in 30 days, more than 10 times the normal cooling rate at that time of year (Fig. 5). The El Niño was brought to an end, and cold La Niña conditions were established in its place.

**Delayed Oscillator Theory and the 1997–98 El Niño**

According to delayed oscillator theory, which is one of the current paradigms for the ENSO cycle (14), evolution of the climate system in the tropical Pacific on interannual time scales is governed by the interplay between large-scale equatorial ocean wave processes and ocean-atmosphere feedbacks. This theory predicts that a buildup of heat content in the western Pacific, mediated by trade wind–forced downwelling equatorial Rossby waves, is a precursor of El Niño (15). Reflection of Rossby waves off the western boundary can initiate El Niño events by generating downwelling equatorial Kelvin waves that propagate eastward to cause warming in the equatorial cold tongue. However, there has been considerable debate as to whether delayed oscillator physics as originally con-

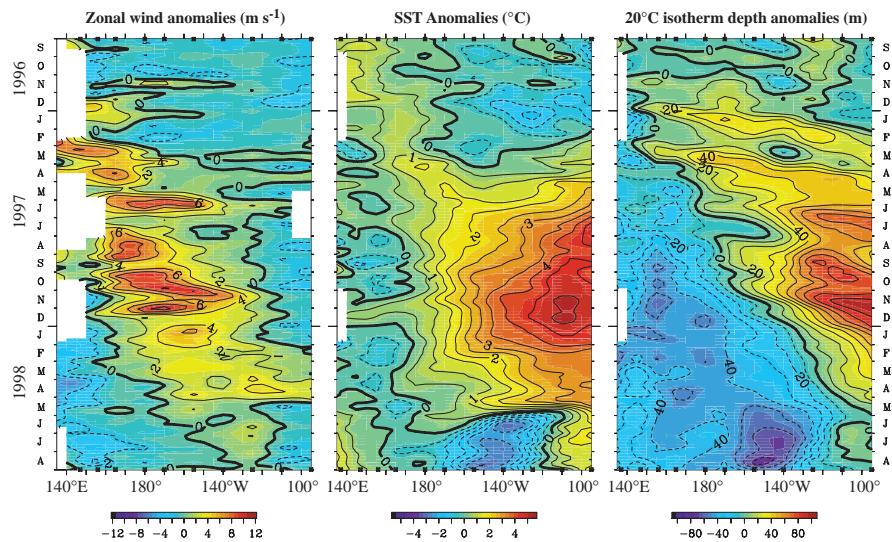


**Fig. 2.** Time versus longitude sections of anomalies in surface zonal wind (left), SST (middle), and 20°C isotherm depth (right) from September 1996 to August 1998. Analysis is based on 5-day averages between 2°N and 2°S of moored time-series data from the TAO array. Anomalies are relative to monthly climatologies that were cubic spline–fitted to 5-day intervals. The monthly SST climatology is based on data from 1950–79 (42). The monthly wind climatology is based on data from 1946–89 (43). The monthly 20°C isotherm depth climatology is based on subsurface temperature data primarily from 1970–91 (44). Positive winds are westerly, and positive 20°C isotherm depths indicate a deeper thermocline. Black squares on the abscissas indicate longitudes where data were available at the start (top) and end (bottom) of the time series.

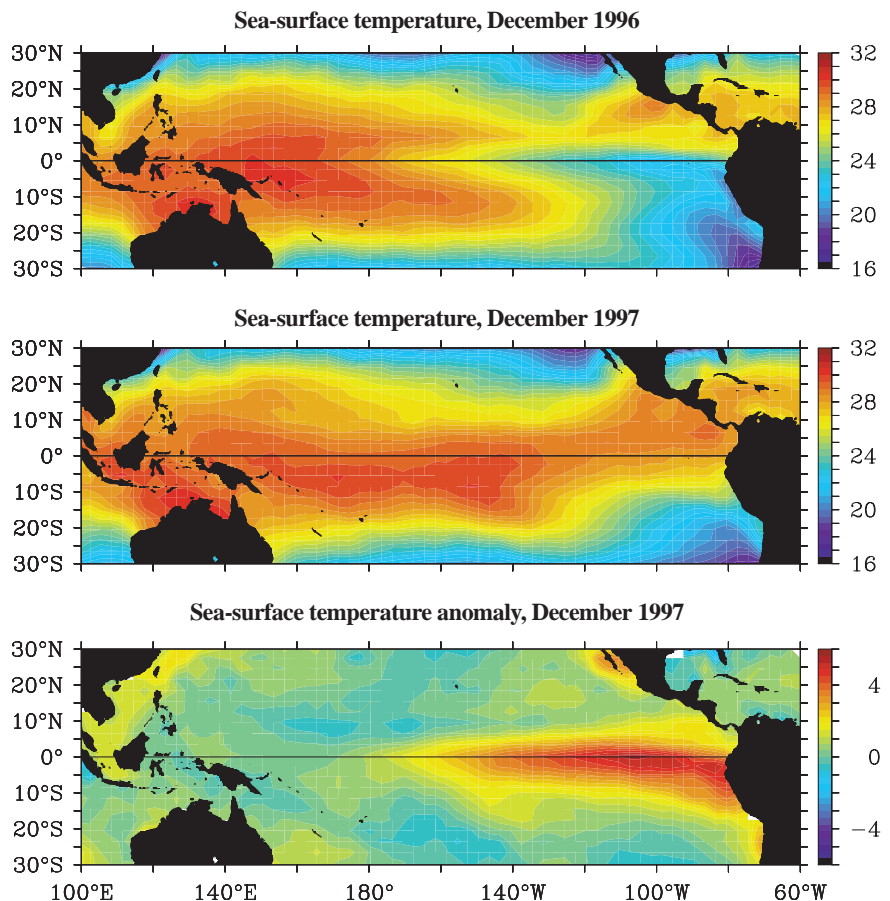


**Fig. 3.** Monthly averaged sea-surface temperature (in degrees Celsius) for December 1996 and December 1997. Monthly average SST anomaly for December 1997 is also shown. The anomaly is relative to the SST climatology referred to in Fig. 2.

Downloaded from www.sciencemag.org on February 6, 2007



ceived can consistently account for the onset of El Niños (16–20). The 1997–98 El Niño affords an opportunity to examine this theory in light of a very strong climate signal that is extraordinarily well defined by new data.

For at least a year before the onset of the 1997–98 El Niño, there was a buildup of heat content in the western equatorial Pacific (Fig. 6) due to stronger than normal trade winds associated with a weak La Niña in 1995–96 (Fig. 2). This buildup of heat content was also associated with unusually warm SSTs west of the date line (Fig. 2). Although these conditions may have set the stage for the development of an El Niño, the onset of the 1997–98 event did not occur until the intensification of the MJO over the western Pacific in late 1996. The MJO goes through a normal seasonal cycle with larger amplitudes in boreal winter and spring. Beginning in late 1996, MJO variations in surface winds amplified even more over unusually warm waters of the western Pacific as these oscillations propagated eastward from the Indian Ocean (21). The oceanic Kelvin waves most evident at the onset of the 1997–98 El Niño were those excited by episodic westerly surface winds associated with the MJO (Figs. 2 and 6). Kelvin waves generated at the western boundary by reflecting Rossby waves were, however, not readily apparent (22).

Delayed oscillator theory also predicts that western boundary wave reflections are important for the termination of El Niño. Rossby waves generated by the collapse of the trade winds at the onset of El Niño are hypothesized to reflect at the western boundary into Kelvin waves, which then propagate eastward to elevate the thermocline in the eastern Pacific. An elevated thermocline creates conditions favorable for surface cooling through local trade wind-driven upwelling. Western boundary reflections of Rossby waves into upwelling Kelvin waves did occur after the onset of the 1997–98 El Niño (12). However, the appearance of easterly wind anomalies in the western Pacific in late 1997 and early 1998 (Fig. 2) also generated upwelling Kelvin waves (22). The development of these easterly anomalies at the height of El Niño, a consistent feature seen in historical data (23), has been interpreted as the response to atmospheric pressure patterns over anomalously cool water as the El Niño evolves (24). Thus, direct wind forcing, in addition to western boundary reflections, preconditioned the ocean for a demise of the El Niño in May–June 1998 (25).

### Implications for Predictability

The 1997–98 El Niño event caught the scientific community by surprise. Several dynamical and statistical ENSO forecast models had success in predicting, one to three seasons in advance, unusually warm tropical

Pacific SSTs for 1997. However, before the onset of the El Niño, model-predicted warmings in virtually every case were much too weak and developed too slowly (4, 26, 27). The first, and heretofore most successful, ENSO forecast model (28) failed to predict the 1997–98 event at all. Conflicting model predictions lead to uncertainty in the forecasting community about what would actually transpire in the tropical Pacific, so that offi-

cial pronouncements of an impending El Niño were not made until April–May 1997 after the first appearance of warm SST anomalies. Once the El Niño was under way, however, predictions of subsequent tropical Pacific SSTs were improved in many cases by initializing the models with highly anomalous observations of prevailing oceanic and atmospheric conditions. These subsequent SST predictions were extremely valuable in mak-

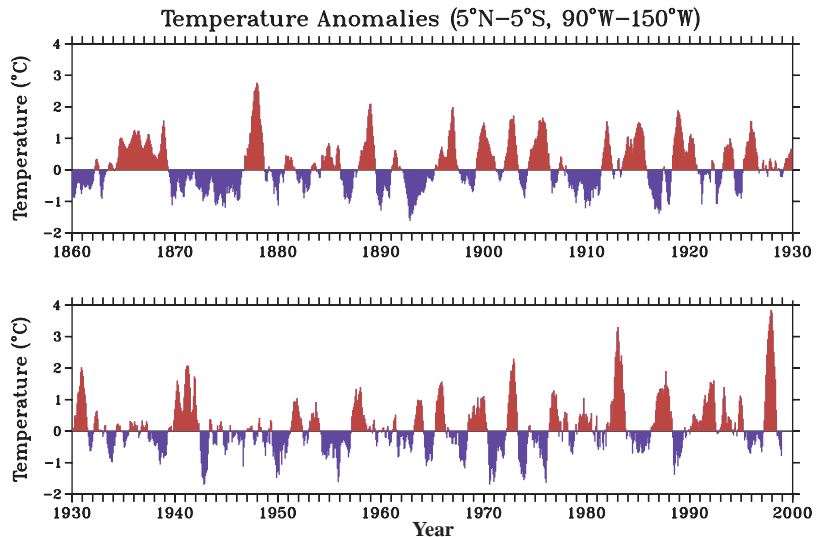


**Fig. 4.** SST anomalies for the region from 5°N to 5°S, 90°W to 150°W from a combination of shipboard data through 1991 and analysis of blended satellite/in situ data afterward. The shipboard data are described in (45), and the blended product is described in (46). Warm anomalies (in red) greater than about 0.5°C generally indicate El Niño events. Cold anomalies (in blue) less than about -0.5°C generally indicate La Niña events.

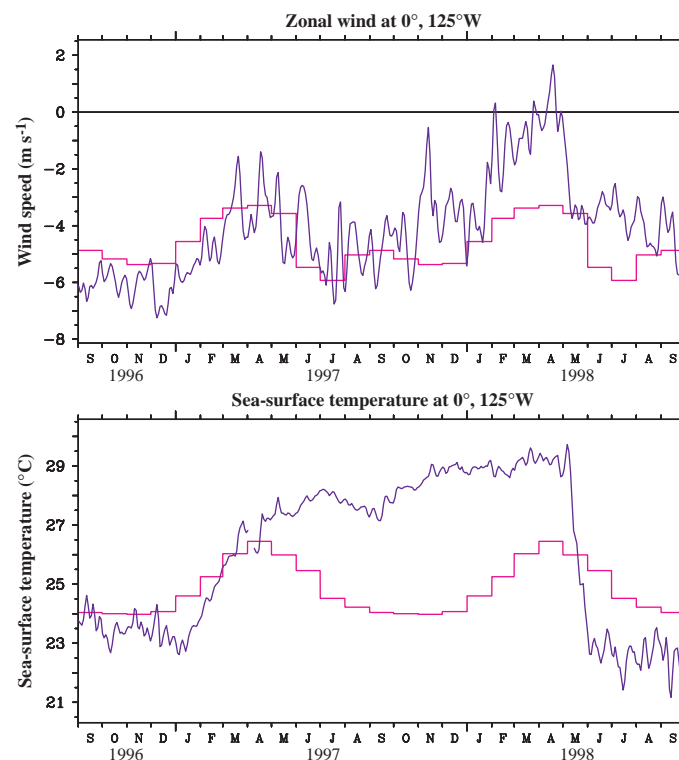


**Fig. 5.** Five-day averaged time series of surface zonal winds and SST from a mooring station on the equator at 125°W. The normal seasonal cycle is shown by magenta lines.

ing long-range weather forecasts for different parts of the globe as the event unfolded (26, 27).

The predictability of ENSO is ultimately linked to large-scale wave dynamics that redistribute upper ocean heat and mass on seasonal to interannual time scales (29). The skill of ENSO forecasting schemes is limited by a number of factors, such as model imperfections, errors in initial conditions, and tendencies toward chaos in the climate system. Moreover, forecast skill is both seasonally and decadal modulated (30). The inability of forecast models to predict the rapid growth of the 1997 El Niño can be attributed to some combination of these factors. With regard to the MJO in particular, most atmospheric circulation models, including those used in dynamical model forecasting schemes, do not simulate intraseasonal variations well, if at all (28, 31). Statistical ENSO forecast models, trained on seasonally averaged conditions over many ENSO cycles, are not particularly sensitive to intraseasonal variations. These models would have difficulty predicting with great accuracy extreme events or abrupt transitions that depended on short time-scale fluctuations. In addition, high-frequency synoptic-scale weather variations are not predict-

able on interannual time scales, so that phenomena like the MJO represent stochastic noise in climate forecasting.

All El Niños from the 1950s to the present have been associated with elevated levels of intraseasonal westerly surface wind forcing (17, 32). In each case, several episodes of westerly wind forcing lasting typically 1 to 3 weeks developed before and during the El Niño events. These winds were related to the MJO or other phenomena such as tropical cyclone formation and cold air outbreaks from higher latitudes. However, episodic wind forcing is not a sufficient condition for El Niños to occur, since such forcing is evident during non-El Niño years as well. It has also been argued that episodic wind forcing is not even a necessary condition for the development of El Niños, since many coupled ocean-atmosphere models simulate ENSO-like variability without it. Nonetheless, theoretical studies indicate that stochastic forcing can amplify and markedly alter the evolution of the ENSO cycle if it occurs on time and space scales to which the ocean is sensitive, and when background oceanic and atmospheric conditions are conducive to the rapid growth of random disturbances (33, 34). Part of the reason for irregularity in the ENSO cycle in terms of frequency, duration, and amplitude of warm and cold events may therefore be attributed to the nonlinear interaction of higher frequency weather variability with lower frequency ocean-atmosphere dynamics (35).

In late 1996, the equatorial Pacific was primed for an El Niño to occur with the buildup of heat content in the western Pacific over the previous 12 to 18 months. It is likely that those forecast models that predicted a warm event prior to its onset were sensitized to precursors associated with this buildup, consistent with delayed oscillator physics. However, the observations suggest that the sudden onset and large amplitude of the 1997–98 El Niño event were at least in part related to forcing by intraseasonal atmospheric oscillations which triggered the eruption of intense warm SST anomalies not foreseen by any forecast model.

Termination of the 1997–98 El Niño was preconditioned by low-frequency ocean wave processes which elevated the thermocline in the central and eastern Pacific. Corresponding to this evolving subsurface thermal structure, many forecast models by late 1997 were calling for a return to normal conditions in mid- to late 1998, and some of these models predicted further development of La Niña conditions (3, 27). The suddenness of the trade-wind intensification which brought the event to an end in May–June 1998, however, was not anticipated by any ENSO forecasting scheme. What caused the trade winds to abruptly intensify is also not known, but they

triggered explosive surface cooling by upwelling cold water from the very shallow thermocline. The intensity of the ensuing SST drop made for a spectacular finale to the 1997–98 El Niño.

Other factors that may have influenced the evolution of the 1997–98 El Niño include interactions with naturally occurring decadal time-scale fluctuations and global warming trends (36–38). The Pacific Decadal Oscillation (39), for example, has been in a warm phase since the mid-1970s, elevating temperatures in the tropical Pacific and affecting the background conditions on which ENSO events develop. The MJO itself has undergone decadal time-scale modulations and is more active since the late 1970s in association with a systematic warming of the Indian Ocean (40). Similarly, following a century-long trend of rising global temperatures, 1998 and 1997 were, in that order, the warmest years on record (41). Corresponding to these climatic changes, there have been more El Niños than La Niñas since the mid-1970s, the early 1990s was a period of extended warmth in the tropical Pacific (18, 36), and the extremely strong 1997–98 El Niño followed by only 15 years the previous record-setting El Niño of 1982–83 (Fig. 4). Exactly how these various phenomena spanning intraseasonal to centennial time scales interact with one another and with ENSO is not entirely clear. Further research is therefore required to better understand the multiscale interactions that potentially affect the ENSO cycle, and to translate that understanding into improved climate forecasting capabilities.

#### References and Notes

1. The ENSO cycle is an irregular oscillation of the climate system with a period of roughly 3 to 4 years. It consists of a warm phase, El Niño, and a cold phase, La Niña.
2. National Research Council, *Accomplishments and Legacies of the TOGA Program* (National Academy Press, Washington, DC, 1996); M. J. McPhaden et al., *J. Geophys. Res.* **103**, 14169 (1998).
3. R. A. Kerr, *Science* **280**, 522 (1998).
4. K. E. Trenberth, *CLIVAR-Exchanges* **3**, 4 (1998).
5. M. J. McPhaden, *Bull. Am. Meteorol. Soc.* **76**, 739 (1995).
6. At some locations along the Peru coast, surface temperature anomalies peaked at 8° to 9°C above normal between December 1997 and March 1998 (Climate Analysis Center, U.S. Department of Commerce, Climate Diagnostics Bulletin, May 1998, Washington, DC).
7. R. A. Madden and P. R. Julian, *J. Atmos. Sci.* **29**, 1109 (1972); K.-M. Lau and P. H. Chan, *Bull. Am. Meteorol. Soc.* **67**, 533 (1986); C. Jones, D. E. Waliser, C. Gautier, *J. Clim.* **11**, 1057 (1998).
8. F. P. Chavez, P. G. Strutton, M. J. McPhaden, *Geophys. Res. Lett.* **25**, 3543 (1998).
9. G. S. E. Lagerloef, G. T. Mitchum, R. Lukas, P. P. Niiler, in preparation.
10. Advection of the eastern edge of the warm pool was also an important feature of previous El Niño events [M. J. McPhaden and J. Picaut, *Science* **250**, 1385 (1990); J. Picaut and T. Delcroix, *J. Geophys. Res.* **100**, 18393 (1995); J. Picaut, M. Ioualalen, C. Menkes, T. Delcroix, M. J. McPhaden, *Science* **274**, 1486 (1996)]. Details of how high-frequency wind forcing can rectify into low-frequency eastward expansion of the

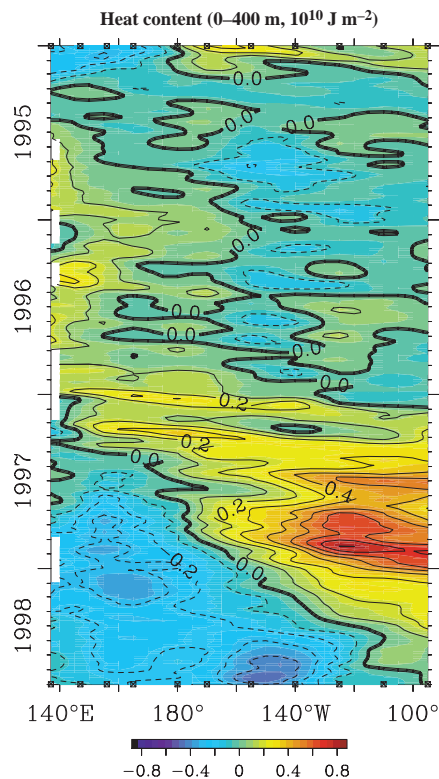


**Fig. 6.** Observed heat content anomalies (from 0 to 400 m depth) averaged between 2°N and 2°S from the TAO array. Temporal resolution is 5 days and contour interval is  $0.1 \times 10^{10} \text{ J m}^{-2}$ . Heat content anomalies are relative to the subsurface temperature climatology referred to in Fig. 2.

- warm pool were described in W. S. Kessler, M. J. McPhaden, and K. M. Weickmann [*J. Geophys. Res.* **100**, 10613 (1995)].
11. W. S. Kessler and M. J. McPhaden, *Deep-Sea Res. Part 2* **42**, 295 (1995); T. P. Barnett, M. Latif, E. Kirk, E. Roeckner, *J. Clim.* **4**, 487 (1991).
  12. J.-P. Boulanger and C. Menkes, *Clim. Dyn.*, in press.
  13. R. A. Weller and S. P. Anderson, *J. Clim.* **9**, 1959 (1996); M. Cronin and M. J. McPhaden, *J. Geophys. Res.* **102**, 8533 (1997); K. E. Brainerd and M. C. Gregg, *ibid.*, p. 10437; J. S. Godfrey *et al.*, *ibid.* **103**, 14395 (1998).
  14. D. Battisti, *J. Atmos. Sci.* **45**, 2889 (1988); M. J. Suarez and P. S. Schopf, *ibid.*, p. 3283; P. S. Schopf and M. J. Suarez, *ibid.*, p. 549.
  15. This aspect of delayed oscillator theory was anticipated by K. Wyrtki [*J. Phys. Oceanogr.* **5**, 572 (1975)].
  16. N. J. Mantua and D. Battisti, *ibid.* **24**, 691 (1994); B. Li and A. J. Clarke, *ibid.*, p. 681.
  17. W. S. Kessler and M. J. McPhaden, *J. Clim.* **8**, 1757 (1995).
  18. L. Goddard and N. E. Graham, *J. Geophys. Res.* **102**, 10423 (1997).
  19. J.-P. Boulanger and C. Menkes, *ibid.* **100**, 25041 (1995); J.-P. Boulanger and L.-L. Fu, *ibid.* **101**, 16361 (1996).
  20. Y. Wakata and E. S. Sarachik, *J. Phys. Oceanogr.* **21**, 434 (1991).
  21. B. Wang and X. Xie [*J. Clim.* **11**, 2116 (1998)] have shown theoretically how the MJO can amplify over warm surface water through ocean-atmosphere interactions. L. Yu and M. M. Reinecker [*Geophys. Res. Lett.* **25**, 3537 (1998)] also present evidence that cold air outbreaks from East Asia and the western North Pacific contributed to the intensification of the MJO at the beginning of the 1997–98 El Niño.
  22. M. J. McPhaden and X. Yu [*Proceedings of the Second Hayes Symposium on Seasonal-to-Interannual Climate Variability—1997/1998 ENSO Cycle*, Dallas, TX, 10 to 15 January 1999 (American Meteorological Society, Boston, MA, 1999), pp. 38–42] use a wind-forced model to compare boundary versus wind-forced Kelvin wave amplitudes during the onset and termination phase of the 1997–98 El Niño. During the onset phase, directly wind-forced downwelling Kelvin waves were about 10 times larger than those generated at the western boundary by reflecting Rossby waves. During the termination phase, boundary versus wind-forced upwelling Kelvin waves were of similar amplitudes.
  23. E. M. Rasmusson and T. H. Carpenter, *Mon. Weather Rev.* **110**, 354 (1982).
  24. R. H. Weisberg and C. Wang, *Geophys. Res. Lett.* **24**, 779 (1997); D. A. Mayer and R. H. Weisberg, *J. Geophys. Res.* **103**, 18635 (1998).
  25. J. Picaut, F. Masia, and Y. du Penhoat [*Science* **277**, 663 (1997)] have suggested that zonal advection associated with eastern boundary-generated Rossby waves may be important in producing ENSO SST anomalies. These Rossby waves result from the reflection of incoming equatorial Kelvin waves along the coast of South America. For the 1997–98 event, eastern boundary reflections appear to be of secondary importance during the onset phase, given the strength of direct wind forcing along the equator. Similarly, termination of the El Niño was related more to the sudden trade wind-driven upwelling of cold water from below the surface rather than wave-related zonal advection of cool water from the east. Zonal advection due to boundary-generated Rossby waves would have brought warmer rather than colder water from the east in early 1998, because the normal east-west SST gradient along the equator was reversed at that time. Once the surface cooling was underway, however, wave-related zonal advection from eastern boundary reflections may have contributed to the westward spreading of cold SST anomalies evident in Fig. 2.
  26. D. L. T. Anderson and M. K. Davey, *Weather* **53**, 295 (1998).
  27. A. G. Barnston, M. H. Glantz, Y. He, *Bull. Am. Meteorol. Soc.*, in press.
  28. M. A. Cane, S. C. Dolan, S. E. Zebiak, *Nature* **321**, 827 (1986).
  29. M. Latif *et al.*, *Clim. Dyn.* **9**, 167 (1994); A. J. Busalacchi, in *Modern Approaches to Data Assimilation in Ocean Modeling* (Elsevier, Amsterdam, 1996), pp. 235–270; M. Ji and A. Leetmaa, *Mon. Weather Rev.* **125**, 742 (1997).
  30. M. A. Balmaseda, M. K. Davey, D. L. T. Anderson, *J. Clim.* **8**, 2705 (1995); D. Chen, S. E. Zebiak, A. J. Busalacchi, M. A. Cane, *Science* **269**, 1699 (1995).
  31. J. M. Slingo *et al.*, *Clim. Dyn.* **12**, 325 (1996).
  32. D. S. Luther, D. E. Harrison, R. A. Knox, *Science* **222**, 327 (1983); D. E. Harrison and B. S. Geise, *J. Geophys. Res.* **96**, 3221 (1991); M. J. McPhaden and S. P. Hayes, *ibid.* **95**, 13195 (1990); S. Verbeek, *Weather* **53**, 282 (1998).
  33. C. Penland and P. D. Sardashmuk, *J. Clim.* **8**, 1999 (1995); B. Blanke, J. D. Neelin, D. Gutzler, *ibid.* **10**, 1473 (1997); Y.-Q. Chen, D. S. Battisti, T. N. Palmer, J. Barsugli, E. S. Sarachik, *Mon. Weather Rev.* **125**, 831 (1997).
  34. A. M. Moore and R. Kleeman, *J. Clim.*, in press.
  35. Another interpretation of irregularity in the ENSO cycle invokes chaos theory and nonlinear interactions of ENSO with the mean seasonal cycle [E. Tziperman, L. Stone, H. Jarosh, M. A. Cane, *Science* **264**, 72 (1994); F.-F. Jin, J. D. Neelin, M. Ghil, *ibid.*, p. 70 (1994); P. Chang, L. Ji, B. Wang, T. Li, *J. Atmos. Sci.* **52**, 2353 (1995)].
  36. K. E. Trenberth and T. J. Hoar, *Geophys. Res. Lett.* **23**, 57 (1996).
  37. M. Latif, R. Kleeman, C. Eckert, *J. Clim.* **10**, 2221 (1997).
  38. K.-M. Lau and H. Weng, *ibid.* in press.
  39. N. J. Mantua, S. R. Hare, Y. Zhang, J. M. Wallace, R. C. Francis, *Bull. Am. Meteorol. Soc.* **78**, 1069 (1997).
  40. J. M. Slingo, D. P. Rowell, K. R. Sperber, F. Nortley, *Q. J. R. Meteorol. Soc.*, in press.
  41. Global mean temperatures generally rise by a few tenths of a degree Celsius following the peak warming of El Niño events, due to losses of heat from the tropical Pacific Ocean to the overlying atmosphere [J. R. Christy and R. T. McNider, *Nature* **367**, 325 (1994); E. K. Schneider, R. S. Lindzen, B. P. Kirtman, *J. Atmos. Sci.* **54**, 1349 (1997)]. The rise in global mean temperatures in 1997–98 was therefore most likely augmented by the occurrence of the extreme 1997–98 El Niño.
  42. R. W. Reynolds and T. M. Smith, *J. Clim.* **8**, 1571 (1995).
  43. S. D. Woodruff, R. J. Slutz, R. L. Jenne, P. Steurer, *Bull. Am. Meteorol. Soc.* **68**, 1239 (1987).
  44. W. S. Kessler, *J. Geophys. Res.* **95**, 5183 (1990); \_\_\_\_\_ and J. P. McCreary, *J. Phys. Oceanogr.* **23**, 1192 (1993).
  45. A. Kaplan *et al.*, *J. Geophys. Res.* **103**, 18567 (1998).
  46. R. W. Reynolds and T. M. Smith, *J. Clim.* **7**, 929 (1994).
  47. The TAO Array is maintained through a multinational partnership involving institutions in the United States (NOAA), Japan (Japan Marine Science and Technology Center), Taiwan (National Taiwan University), and France (Institut de Recherche pour le Développement, formerly the Institut Français de Recherche pour le Développement en Coopération). Production of this manuscript was supported by NOAA's Environmental Research Laboratories. This paper is contribution number 2029 from NOAA/Pacific Marine Environmental Laboratory and 665 from the University of Washington Joint Institute for the Study of the Atmosphere and the Ocean.

# Tired of waiting for Godot?

NEW! *Science* Online's Content Alert Service: Now you can get *instant* summaries of science news and research findings with *Science's* Content Alert Service. This free enhancement to your *Science* Online subscription delivers e-mail summaries of the latest news and research articles published each Friday in *Science* – *instantly*. To sign up for the Content Alert service, go to *Science* Online and end the wait.

**Science**  
www.sciencemag.org

For more information about Content Alerts go to [www.sciencemag.org](http://www.sciencemag.org). Click on Subscription button, then click on Content Alert button.